A de Haas-van Alphen study of the Fermi surfaces of superconducting LiFeP and LiFeAs

C. Putzke,[1] A.I. Coldea,[2,*] I. Guillamón,[1] D. Vignolles,[3] A. McCollam,[4] D. LeBoeuf,[3] M.D. Watson,[2] I.I. Mazin,[5] S. Kasahara,[6] T. Terashima,[6] T. Shibauchi,[7] Y. Matsuda,[7] and A. Carrington[1,†]

[1] *H.H. Wills Physics Laboratory, University of Bristol, Tyndall Avenue, Bristol, BS8 1TL, UK.*
[2] *Clarendon Laboratory, Department of Physics, University of Oxford, Parks Road, Oxford OX1 3PU, U.K.*
[3] *Laboratoire National des Champs Magnétiques Intenses (CNRS), Toulouse, France.*
[4] *High Field Magnet Laboratory, IMM, Radboud University Nijmegen, 6525 ED Nijmegen, The Netherlands.*
[5] *Code 6393, Naval Research Laboratory, Washington, DC 20375, USA.*
[6] *Research Center for Low Temperature and Materials Sciences, Kyoto University, Sakyo-ku, Kyoto 606-8501, Japan.*
[7] *Department of Physics, Kyoto University, Sakyo-ku, Kyoto 606-8502, Japan.*

(Dated: July 25, 2011)

We report a de Haas-van Alphen (dHvA) oscillation study of the 111 iron pnictide superconductors LiFeAs with $T_c \approx 18$ K and LiFeP with $T_c \approx 5$ K. We find that for both compounds the Fermi surface topology is in good agreement with density functional band-structure calculations and shows quasi-nested electron and hole bands. This disagrees with photoemission results for LiFeAs. The effective masses generally show significant enhancement, up to ~ 3 for LiFeP and ~ 5 for LiFeAs. However, one hole Fermi surface shows a very small enhancement in LiFeP whereas the same sheet has significant enhancement in LiFeAs. This difference probably results from $\boldsymbol{k}$-dependent coupling to spin fluctuations and may explain the nodal and nodeless structure of the superconducting gap in LiFeP and LiFeAs respectively.

Identification of the particular structural and electronic characteristics that drive superconductivity in the iron-based materials continues to be a central experimental and theoretical question in the field. A successful theory needs to explain trends, such as the variation of T_c and also the structure of the superconducting energy gap. In most of the iron arsenides the parent materials have a non-superconducting, antiferromagnetically ordered ground state. Disruption of this magnetic order leads to superconductivity and then eventually a non-superconducting paramagnetic ground state. A good example is the $BaFe_2(As_{1-x}P_x)_2$ series which has a maximum T_c =30 K when $x \simeq 0.33$ [1, 2]. Here $BaFe_2As_2$ has a magnetic ground state whereas $BaFe_2P_2$ is a paramagnet and neither superconduct.

The 111-family of iron-pnictides $LiFeAs_{1-x}P_x$, is unique because both LiFeAs and its counterpart LiFeP superconduct and are non-magnetic with $T_c \sim 18$ K [3, 4] and ~ 5 K [5], respectively. Also, penetration depth measurements have shown that LiFeAs is fully gapped [6, 7], whereas LiFeP has gap nodes [7]. Establishing whether this switch of pairing structure is linked to changes in the topology of the Fermi surface (FS) will provide an excellent test of candidate theories for the superconducting pairing in these materials. It was claimed, based on the angle resolved photoemission (ARPES) data [8], that the fermiology in LiFeAs is very different from the predictions from density functional theory (DFT), in particular, there is no quasi-nesting between the hole and electron FS pockets. In this Letter, we present a study of the de Haas-van Alphen effect in both LiFeP and LiFeAs which establishes the topology of the *bulk* Fermi surface which we find is in good agreement with the DFT calculations. We find significant orbit dependence to the

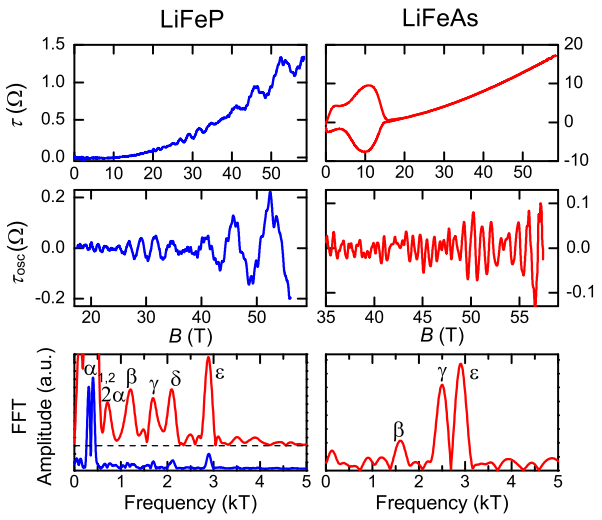

FIG. 1. (color online) Torque versus field for LiFeP and LiFeAs at $T = 1.5$ K. The top panels show the raw torque data in units of the change in the cantilever resistance. The middle panel shows the oscillatory part of the torque after subtraction of a smooth background. The bottom panel shows the fast Fourier transform (FFT) of the torque. For the peak labels see the main text. For LiFeP we show FFT spectra computed over two different field windows. The lower curve uses a wide field window (25-58 T) which shows the splitting of the α peaks, whereas the upper curve uses a smaller high field window (40-58 T) which decreases the influence of noise on the higher frequency peaks (dashed line represents zero for the upper curve).

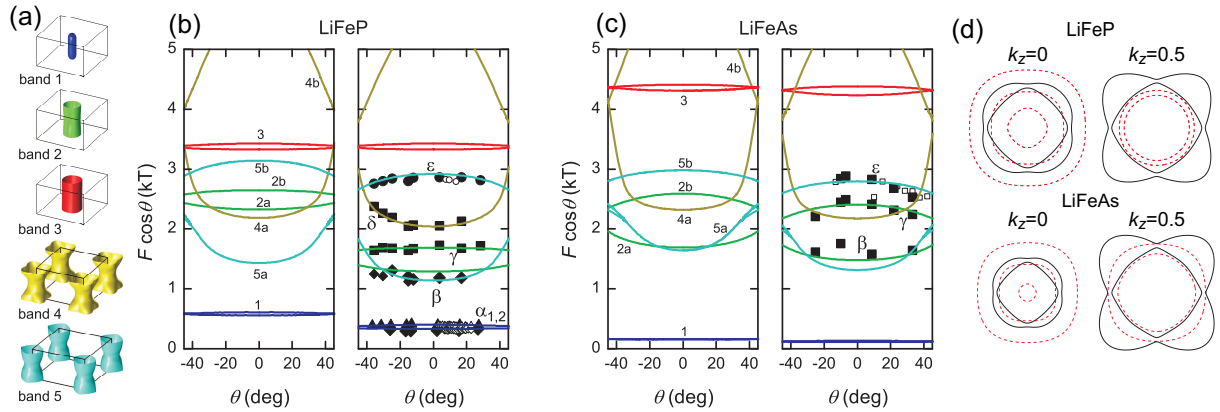

FIG. 2. (color online) (a) Calculated Fermi surfaces of LiFeP. (b) and (c) Show the evolution of de Haas-van Alphen frequencies with magnetic field angle. Experimental data are shown in the right panels as symbols (solid symbols = pulsed field, open symbols are for different samples in dc field). The solid lines show the result of the DFT calculations; the bands are shifted in the right hand panels to best fit the experimental results. The numbers refer to the bands in (a). In all panels the frequencies have been multiplied by $\cos\theta$ for clarity. (d) Slices through the determined Fermi surfaces at particular k_z values (with shifted bands). The dashed/solid lines are the hole/electron sheets respectively, and the latter have been shifted so their center coincides with the holes.

mass enhancement factors which we argue are linked to the contrasting superconducting gap structures and T_c in these compounds.

Single crystals of LiFeP and LiFeAs were grown by a flux method [9]. Small single crystals, typically $50\times50\times10\,\mu\mathrm{m}^3$ for LiFeP and $100\times200\times50\,\mu\mathrm{m}^3$ for LiFeAs, were selected for the torque measurements. To avoid reaction with air the samples were encapsulated in degassed Apiezon-N grease. Sharp superconducting transitions were measured using radio frequency susceptibility with T_c onset (midpoint) values of 4.9 K (4.7 K) and 18.4 K (17.3 K) for LiFeP and LiFeAs, respectively. The samples were mounted onto miniature Seiko piezo-resistive cantilevers which were installed on a rotating platform, immersed in liquid ^{4}He, in the bore of a pulsed magnet in Toulouse. Measurements were also conducted in an 18 T superconducting magnet in Bristol and a 33 T Bitter magnet in Nijmegen equipped with ^{3}He refrigerators.

Torque vs. magnetic field data are shown in Fig. 1. For both materials de Haas-van Alphen oscillations are seen at high fields, particularly after subtraction of a low order polynomial background (see Fig. 1 middle panels). After the fast Fourier transform (FFT) as a function of inverse field, several strong peaks are visible (Fig. 1), which correspond to the extremal cross-sectional areas A_k of the FS: $F=\hbar A_k/2\pi e$. For LiFeP, the spectrum is dominated by two low dHvA frequencies around 300 T and 400 T, labelled α_1 and α_2. The amplitude and frequency of the peak at ~ 750 T is consistent with this being the second harmonic of the α peaks. The other four peaks $(\beta,\gamma,\delta,\varepsilon)$ are clearly derived from unique Fermi surface orbits. The α and ε peaks were also observed for three other samples. For LiFeAs, three frequencies are visible $\beta,\gamma,\varepsilon)$. The γ and ε peaks were also seen on two other samples.

To properly identify these FS orbits, we performed field sweeps with different field orientations starting from $\theta=0^\circ$ $(B\|c)$ and rotating towards the ab-plane. For a perfectly two dimensional (2D) FS, $F\propto 1/\cos\theta$, so by multiplying F by $\cos\theta$ the degree of two dimensionality of a FS can be easily seen. For quasi-2D surfaces, $F\cos\theta$ will decrease with increasing θ for a local maximum of Fermi surface orbit area as a function of k_z whereas the opposite will be true for a local minimum. The data in Fig. 2 suggest that for LiFeP ε is a maximum, β and δ are minima, and γ is from a very 2D section. The two lowest frequency α orbits have opposite curvature indicting that they are the maximum and minimum of the same FS sheet. For LiFeAs, ε and γ orbits are maxima, while the noise level for the β orbits is too high to make definitive conclusions.

To identify the origin of the orbits and solve the structure of the Fermi surface we have performed DFT calculations using the linear augmented plane wave method, implemented in the WIEN2K package [10]. We used the experimental crystal structure [11] and included spin-orbit coupling (SOC). The calculated Fermi surfaces (see Fig. 2(a,d)) are quite similar for both materials, there are three hole bands at Γ and two electron bands at M as found previously [12]. The two outermost hole sheets are quite 2D, whereas the innermost xz/yz hole pocket is strongly hybridized with d_{z^2} near Z and is closed there, while remaining 2D away from this point. By contrast, the electron orbits are very strongly warped. This geometry is reflected in the calculated angular dependence of the dHvA orbits (Fig. 2(b,c)). For the 2D hole sheets $F\cos\theta$ varies little with angle and the maximal and minimal area are close. For the electron sheets there is a large

deviation from this behavior. For LiFeP, SOC splits the two outermost hole bands, which are accidentally nearly degenerate in non-relativistic calculations, and causes their character to be mixed $d_{xz/yz}/d_{xy}$. In LiFeAs these bands are well separated irrespective of SOC and have a predominantly $d_{xz/yz}$ (middle) and d_{xy} (outermost) character. The SOC also splits the electron bands along the zone edge (X-M) inducing a gap of $\sim$35 meV (see 2(d)), hence as in LaFePO [13] we estimate that magnetic breakdown orbits, along the elliptic electron surfaces in the unfolded Brillouin zone, to be strongly damped.

By comparing the calculations to the data (Fig. 2(b,c)), in particular the curvature of $F\cos\theta$, the correspondence between the observed dHvA frequencies and the predicted Fermi surface orbits is immediately apparent. For LiFeP, relatively small shifts (somewhat smaller than for other Fe pnictides) of the band energies: +35 meV and +20 meV for band 4 and 5 (electron) and −60, −73 meV for bands 1 and 2 (hole) bring the observations and calculations into almost perfect agreement as shown in Fig. 2(b). As in other Fe pnictides [14], these shifts shrink the FSs. For band 3, the electron count suggests that if it shifts, it shifts little, and remains large ($\sim$ 3.5 kT), which is probably why it was not observed in our experiment. Indeed if the mean free path for that band is about the same as for other hole bands, its larger size would suppress the signal below the noise level. Similarly, the maximal orbit of band 4 is close to 6 kT and was also not observed. On the contrary, the strong signals for the smallest α orbits are due to their small size and strongly 2D shape – both of these factors enhance the dHvA torque signal. We also can see that the observed β frequencies are likely a mixture of signals from orbits 2a (hole) and 5a (electron) which are not separately resolved.

For LiFeAs, the curvature and absolute values of $F\cos\theta$ suggest that the ε orbit originates from the maximum of the inner electron Fermi surface (band 5) and the γ orbit from the maximum of the middle hole surface (band 2). The β orbit probably originates from a mixture of the minima from these two bands. To exactly match the data with the calculations only very small shifts of the band energies are required (+20 meV for the electron bands and −7 meV for the holes) (Fig. 2(b)). Importantly, the very small band 1 FS was not observed, even though the same band gave the largest signals for LiFeP. This suggests that band 1 does not cross the Fermi level in LiFeAs, which requires that it shifts down by ~ -40 meV, possibly because of enhanced SOC.

The strength of the electron-electron interactions can be estimated from measurements of the quasiparticle effective mass m^* on each orbit through the temperature dependence of the amplitude of the dHvA signals, by fitting the latter to the Lifshitz-Kosevich formula [15] (Fig. 3). These measurements were conducted in dc field on the same samples to avoid any possibility of sample heating at low temperature. The derived values along with the DFT calculations are shown in Table I.

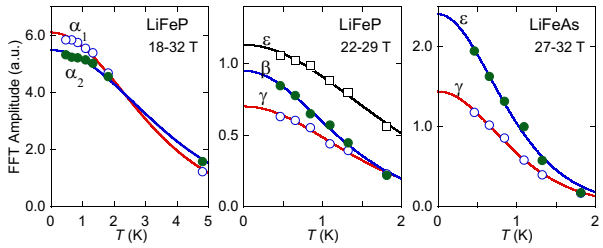

FIG. 3. (color online) Quasiparticle effective masses determination. Amplitude of the FFT peaks (the field ranges as indicated) vs. T. The lines are fits to the Lifshitz-Kosevich formula [15]. The effective mass values are shown in Table I.

TABLE I. Measured and calculated dHvA frequencies. The measured frequencies are extrapolated to $\theta = 0$. The effective (m^*) and calculated (m_b) band masses are quoted in units of the free electron mass (− sign indicates hole orbit). For the value marked † there is additional uncertainty in m^*/m_b as the observed FFT peak likely originate from overlapping electron and hole orbits (see text). The masses for the δ(LiFeP) and β (LiFeAs) orbits could not be determined accurately due to signal to noise issues.

LiFeP						
DFT calculation			Experiment			
Orbit	$F(T)$	m_b	Orbit	$F(T)$	m^*	$m^*/m_b - 1$
1_a	557	−0.48	α_1	297(5)	1.17(5)	1.4(1)
1_b	607	−0.46	α_2	400(3)	1.00(5)	1.2(1)
2_a	2325	−1.7				
2_b	2645	−1.6	γ	1677(10)	2.6(2)	0.6(2)
3_a	3328	−1.8				
3_b	3428	−1.6				
4_a	2183	+0.87	δ	2042(12)		
4_b	6014	+1.8				
5_a	1430	+1.0	β	1180(30)	3.0(2)	2.0(2)†
5_b	3142	+0.77	ε	2858(40)	2.0(2)	1.6(2)
LiFeAs						
DFT calculation			Experiment			
Orbit	$F(T)$	m_b	Orbit	$F(T)$	m^*	$m^*/m_b - 1$
1_a	130	−0.31				
1_b	149	−0.23				
2_a	1585	−2.11				
2_b	2529	−1.50	γ	2400(25)	4.6(2)	2.1(1)
3_a	4402	−2.11				
3_b	4550	−2.12				
4_a	2359	+1.22				
4_b	6237	+2.34				
5_a	1584	+1.54	β	1593(10)		
5_b	2942	+0.99	ε	2800(40)	4.8(2)	3.9(2)

For LiFeP, the enhancements factors $\lambda = m^*/m_b - 1$ vary strongly between orbits. For the electron sheet (band 5) $\langle\lambda\rangle \simeq 1.8$, which is comparable to values found for the electron sheets of LaFePO (T_c=6 K) [16]. The small hole orbits ($\alpha_{1,2}$) are also strongly enhanced, however for the larger hole orbit (orbit γ, band 2) λ is ~ 3 times smaller than for the electrons, despite having similar orbital character. As an enhancement $\lambda \simeq 0.2$ [17] is expected from electron-phonon coupling, this means that the residual electron-electron component for this orbit is very weak. This is an interesting observation, relevant to the ongoing discussion [18] as to whether the mass enhancement comes entirely from local correlations or partially from long range spin fluctuations. If the mass renormalization in this compound is due to the same spin fluctuations that are believed to cause superconductivity, we can conclude that band 2 is very weakly coupled with these fluctuations, so that the pairing amplitude on this band will be small and hence it is a possible candidate for the location of the gap nodes. RPA and functional RG calculations suggest [18] that node formation is controlled by the xy pocket, so that if this pocket exists, the order parameter is nodeless, otherwise nodes form on an *electron* (band 4, in our notation) pocket. LiFeP seems to deviate from this rule, as it has a well developed xy pocket (band 3). LiFeP therefore appears to be a challenging and an extremely interesting material for further theoretical modelling.

For LiFeAs, the measured effective masses are uniformly larger than in LiFeP. For the electron sheet (band 5) λ is more than 2 times larger than in LiFeP. Interestingly, λ for the γ orbit, which was small in LiFeP, is $\sim$3 times larger in LiFeAs. Both of these observations are in line with the idea that mass renormalization is caused *by the same interaction that drives superconductivity*, since LiFeAs both has a higher T_c and no nodes.

A determination of the Fermi surface of LiFeAs using ARPES has been reported by Borisenko *et al.* [8]. They found that the Fermi surface was quite different from that calculated in DFT, in particular that there were two hole sheets with very different area, not matching the electron sheets. They concluded that there is almost no nesting present. A detailed comparison to our data shows that their electron bands are in reasonable agreement with ours in terms of cross-sections but there appears to be significant differences in the hole bands. Our data show that the inner electron (band 5) and middle hole band (band 2) are very close in size and shape (see Fig. 2) and hence are quasi-nested. The discrepancy could be due to surface effects in the photoemission measurements.

In summary, dHvA oscillations have been observed in two members of the 111 family of superconductors, LiFeP and LiFeAs. In both cases we find that the data are consistent with the DFT calculated Fermi surface. The many-body mass enhancements are larger in LiFeAs than in LiFeP, and in the latter one hole band has hardly any enhancement at all. This correlates with the lower T_c and nodal gap in LiFeP, and suggests that the mass enhancement is to a large extent due to a $\boldsymbol{k}$-dependent spin-fluctuation induced interaction, which is also responsible for the pairing. The general trend of increasing mass enhancement as the As content and T_c increases agrees with results for the $BaFe_2(As_{1-x}P_x)_2$ series [14]. For both LiFeP and LiFeAs the electron and hole Fermi surfaces are of similar size and are close to fulfilling a geometric nesting condition. The main difference in topology between the two materials is that LiFeP has a third small hole Fermi surface which is absent in LiFeAs. The xy pocket believed to be responsible for nodeless superconductivity in other pnictides is present in both compounds. Thus, it remains an open question and a challenge to theories to explain the nodal gap structure in LiFeP.

We thank E. Kampert, F. Wolff-Fabris, E.A. Yelland and F. Fabrizi for technical assistance and S. Borisenko for discussions. This work is supported by EPSRC (UK), EuroMagNET II under the EU contract no. 228043, and by KAKENHI from JSPS.

* corresponding author:amalia.coldea@physics.ox.ac.uk
† corresponding author:a.carrington@bristol.ac.uk

[1] S. Jiang *et al.*, J. Phys. Cond. Mat. **21**, 382203 (2009).
[2] S. Kasahara *et al.*, Phys. Rev. B **81**, 184519 (2010).
[3] J. H. Tapp *et al.*, Phys. Rev. B **78**, 060505 (2008).
[4] M. J. Pitcher *et al.*, Chem. Comm. **45**, 5918 (2008).
[5] Z. Deng *et al.*, EPL **87**, 37004 (2009).
[6] H. Kim, M. A. Tanatar, Y. J. Song, Y. S. Kwon, and R. Prozorov, Phys. Rev. B **83**, 100502 (2011).
[7] K. Hashimoto *et al.*, ArXiv:xxx.xxx.
[8] S. V. Borisenko *et al.*, Phys. Rev. Lett. **105**, 067002 (2010).
[9] S. Kasahara *et al.*, unpublished.
[10] P. Blaha, K. Schwarz, G. K. H. Madsen, D. Kvasnicka, and J. Luitz, *WIEN2K, An Augmented Plane Wave + Local Orbitals Program for Calculating Crystal Properties* (Karlheinz Schwarz, Techn. Universität Wien, Austria, 2001).
[11] The lattice parameters for LiFeP were determined by x-ray diffraction at 300 K, a=3.6955 Å c=6.041 Å $z_{\rm Li}$=0.1437, $z_{\rm P}$=0.2803 and for LiFeAs we used: a=3.7914 Å c=6.3639 Å $z_{\rm Li}$=0.1541, $z_{\rm As}$=0.2635 from Ref [3].
[12] I. R. Shein and A. L. Ivanovskii, Solid State Commun. **150**, 152 (2010).
[13] A. Carrington *et al.*, Physica C **469**, 459 (2009).
[14] H. Shishido *et al.*, Phys. Rev. Lett. **104**, 057008 (2010).
[15] D. Shoenberg, *Magnetic Oscillations in Metals* (Cambridge University Press, Cambridge, 1984).
[16] A. I. Coldea *et al.*, Phys. Rev. Lett. **101**, 216402 (2008).
[17] L. Boeri, O. V. Dolgov, and A. A. Golubov, Physica C **469**, 628 (2009).
[18] P. J. Hirschfeld, M. M. Korshunov, and I. I. Mazin, arXiv:1106.3712.